Electromagnetically induced optical anisotropy of an ultracold atomic medium

V. M. Datsyuk, I. M. Sokolov,* and D. V. Kupriyanov
Department of Theoretical Physics, State Polytechnic University, 195251, St.-Petersburg, Russia

M. D. Havey†
Department of Physics, Old Dominion University, Norfolk, Virginia 23529, USA
(Received 25 September 2007; published 11 March 2008)

We consider radiative transport in ultracold atomic systems under conditions of electromagnetically induced transparency. We calculate the macroscopic susceptibility and scattering tensors of the light and show that essential anisotropic optical properties such as dichroism and birefringence naturally appear. In such a case, light propagation through a spatially nonhomogeneous atomic cloud is considered for an arbitrary direction of the probe light. We determine the polarization properties of the coherently transmitted probe light as well as the polarization dependence of light incoherently scattered in an arbitrary direction. Both the steady state regime and time-dependent case are discussed. Concrete calculations are performed for the case of an inhomogeneous and ultracold sample of ^{87}Rb atoms.

DOI: 10.1103/PhysRevA.77.033823 PACS number(s): 42.50.Gy, 34.50.Rk, 34.80.Qb

I. INTRODUCTION

In the last decade, control of optical properties of matter by means of auxiliary electromagnetic fields has attracted significant scientific and technical attention. Electromagnetically induced atomic coherence changes the optical properties of atomic samples in sometimes dramatic ways, and is responsible for such effects as coherent population trapping, electromagnetically induced transparency, "slow light," and "stopped light," to name a few [1–3]. Interest in these effects is partly determined by their possible applications in several broad fields, including optical communications, atomic timekeeping and atomic memories, light amplification, and lasing without inversion.

Recently, more detailed attention has been paid to polarization phenomena under electromagnetically induced transparency (EIT) in atomic media. Due to optical selection rules and different dipole moments of various atomic transitions, polarized coupling fields act differently on different Zeeman sublevels and consequently disturbs them distinctly. On the one hand, these general conditions lead to a strong influence of coupling light polarization on EIT. On the other, they give the possibility of control of the polarization properties of the probe light by means of such effects as induced dichroism and birefringence.

By now polarization phenomena under EIT have been investigated both for multilevel ladder-type [4–8] and for lambda-type atomic energy level configurations [9–11]. In the past few years, several groups have also experimentally studied the influence of a static magnetic field on the polarization sensitivity of EIT. Particularly, electromagnetically induced magnetochiral anisotropy in a resonant medium has been predicted and experimentally demonstrated in Refs. [12,13]. The influence of a magnetic field on creation and retrieval of polaritonic excitations in stopped light experiments has been considered in Refs. [14,15].

In spite of no apparent lack of publications in this area, some aspects of polarization phenomena under EIT conditions have not been adequately explored. For example, nearly all theoretical studies have been done for a collinear geometry of control and probe light, i.e., in the case when the propagation direction of the fields coincide. At the same time, noncollinear geometry is interesting from several different points of view. First, some experiments on slow light and electromagnetically induced transparency have been done in such geometry, for example, the remarkable investigations of Hau *et al.* [16]. Second, noncollinearity of the pump and probe beams influences the linewidth of the EIT resonance. This is evidently very important for such quantum metrology devices as quantum frequency standards and high precision magnetometers based on narrow EIT resonances [17–19]. Finally, but more generally, we deal with a noncollinear geometry every time we consider incoherent light scattering. In this case, the scattered light can propagate in an arbitrary direction with respect to the control light wave vector even if the initial directions of both fields coincide. Though incoherent scattering can be essential in experiments on EIT (see for example [20–22]) the anisotropic effect in such a case has not been studied in detail. Beyond this, there is in general some loss of incident probe flux of a given initial polarization which appears partly as diffusive light in the medium, and partly as orthogonally polarized light propagating in the initial probe direction. Understanding and disentangling these various components (in the absence of 4π detection and polarization analysis) is one element motivating our current studies.

The main goal of the present paper is to consider in detail optical anisotropy of atomic ensembles under conditions of electromagnetically induced transparency. Within the framework of that goal we will study polarization properties of the light transmitted (coherently forward scattered) through the atomic ensemble in an arbitrary direction with respect to the propagation direction of the control field. We will consider both the steady state regime as well as the response to a temporally pulsed probe beam. We will also investigate the polarization properties of the incoherently scattered light. In

*IMS@IS12093.spb.edu
†mhavey@odu.edu

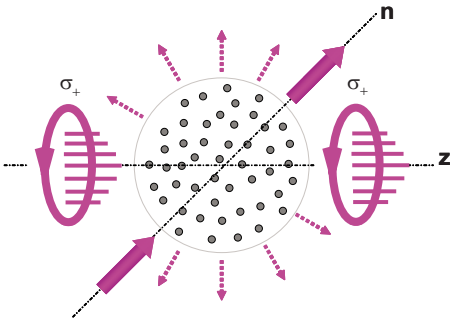

FIG. 1. (Color online) Schematic diagram showing the excitation geometry for observation of the EIT effect in an atomic system. The coupling field is applied with right-handed circular polarization and with a wide aperture to fill the volume where atoms are located. The probe mode with a narrower aperture crosses the atomic ensemble along a selected direction **n**. Part of the probe light is incoherently scattered in all directions.

all calculations we are motivated by ongoing and proposed experiments to consider the case of an ^{87}Rb atomic cloud prepared in magneto-optical trap. This orientation toward close comparison with a common experimental arrangement requires that we take into our theoretical considerations such important aspects as the spatial inhomogeneity of the cloud. As is indicated later in this report, we take a characteristic Gaussian density distribution for the cold atomic cloud [23].

The paper is organized as follows. In Sec. II, we describe our theoretical approach which is suitable for analysis of the polarization effects we consider. We introduce the mesoscopic characteristics of the process, namely, the susceptibility and scattering tensors for light under conditions of EIT. We show that many important features of light propagation can be understood at an analytical level even in the case of spatial inhomogeneity and an anisotropic atomic medium taking into account both hyperfine and Zeeman structure of atomic levels.

In Sec. III we analyze the spectral behavior of dichroism and birefringence of the atomic ensemble. At first we study polarization properties of the transmitted probe light. We show that in the general case this light is modified its original polarization. In the transmitted light there is a polarization component orthogonally polarized with respect to the incoming probe light. We show also that in the case of a temporally Gaussian probe pulse this component has a complicated and structured time dependence. In the remainder of this section we analyze depolarization under incoherent scattering. Both Rayleigh and Raman scattered modes are considered [24].

II. CALCULATION APPROACH

A. Basic assumptions

As a system where optical anisotropy plays an important role under conditions of EIT, we consider a configuration of optical transitions in the hyperfine manifold of the D_1 line of ^{87}Rb. The excitation geometry and the energy level diagram are illustrated in Figs. 1 and 2. A strong coupling field with right-hand circular polarization is applied between the $F=2$

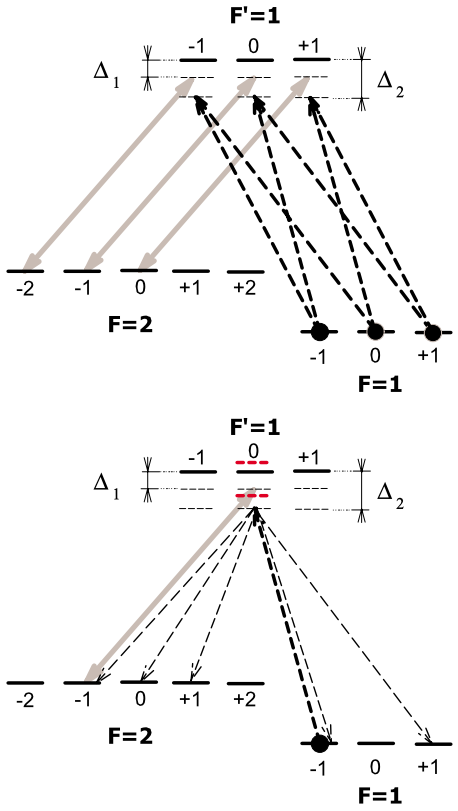

FIG. 2. (Color online) Excitation scheme for observation of the EIT effect in the system of hyperfine and Zeeman sublevels of the D_1 line of ^{87}Rb. The coupling field is applied with right-handed circular polarization to the $F=2\rightarrow F'=1$ transition. The probe mode is applied to $F=1\rightarrow F'=1$ transition and can cause different excitations depending on its polarization and propagation direction. The upper diagram shows the transitions contributing to the susceptibility tensor. Despite homogeneous population of the Zeeman sublevels, the susceptibility tensor becomes essentially anisotropic due to the presence of the coupling field. The lower diagram, in the example of $|m\rangle=|1,-1\rangle\rightarrow|m''\rangle$ transitions, illustrates how the dressing effects, associated with the coupling field, modify the spontaneous scattering of the probe mode. The probe light is scattered from both the components of the Autler-Townes doublet shown by the red-dashed line.

hyperfine sublevel of the ground state and $F'=1$ hyperfine component of the excited level. A weak probe beam is quasiresonant with the $F=1\rightarrow F'=1$ hyperfine transition. All nonlinear optical effects connected with the probe light are assumed to be negligible. In our calculations this field will be taken into account only in the first nonvanishing order.

In contrast to nearly all previous studies of EIT effects for such a configuration, where ideal conditions of the Λ-type configuration are examined and a model of a three level system works ideally, we will consider probe light with arbitrary polarizations and different propagation directions. As illustrated in the upper diagram of Fig. 2, such probe light can cause different Zeeman transitions.

In the calculation we direct our attention to experimental conditions which take place in an atomic ensemble formed in a vapor-loaded magneto-optical trap after the trapping and repumping lasers and the quadrupole magnetic field are

switch off. For the typical conditions of the trap, the Doppler shift is many times smaller than the natural linewidth of the excited state and the interatomic distances on average are much larger than the optical wavelength (dilute medium). This allows us to completely neglect all effects associated with atomic motion, atomic collisions, and sample boundary. Among all relaxation processes we have to take into account only natural spontaneous decay of the excited state, see the lower diagram of Fig. 2.

The detuning of the coupling and probe laser frequencies from the corresponding atomic resonances (Δ_1 and Δ_2, respectively) are assumed to be much less than the hyperfine splitting. This circumstance, along with relatively large hyperfine splitting in the excited state, allows us take into account only one hyperfine sublevels $F'=1$ of this state.

B. The mesoscopic description of light propagation

Light propagation through a dilute atomic cloud under conditions of EIT resonance can be naturally described with the Green's function formalism. This formalism was earlier applied to the problem of light transport through a polarized and ultracold atomic vapor formed in a magneto-optical trap, see Refs. [23,25]. Its generalization for the conditions of two-photon EIT resonance has been recently done in Ref. [22]. Below we briefly discuss the main statements of the Green's function approach, which are important in the context of anisotropy effects induced by the EIT resonance.

The light transport in a dilute medium generally performs a diffusion-type process, which in a semiclassical picture can be visualized as a forwardly propagating wave randomly scattered by medium inhomogeneities. In an optically dense sample this process generates a zigzag-type path consisting of either macroscopically or mesoscopically scaled segments of forwardly propagating waves. The light originally incomes to the sample as a plane wave characterized by a certain aperture and its deflection from the forward propagation, if diffraction is negligible, is only initiated by incoherent scattering events. Mathematically the process can be approached as a solution of macroscopic Maxwell equations, where incoherent scattering is initiated by atoms first excited by incoming wave and then considered as a sources of secondary waves. To entirely simulate the process, the Monte Carlo scheme can be applicable. The forwardly propagating incoming, secondary and multiply scattered waves can be expressed via a retarded-type Green's propagation function. This propagation function is completely described by the macroscopic susceptibility tensor. The incoherent scattering events, which randomly happen in the medium, can be probabilistically simulated and properly described with the scattering theory formalism. In application to the light scattering there is mostly important to define the scattering tensor, which further expresses the amplitude of the process and its cross section. Thus the susceptibility tensor and scattering tensor are two crucial ingredients for Monte Carlo simulation of the diffuse light dynamics in any turbid medium and in an atomic gas in particular.

In Fig. 2 there is shown the energy diagram and the scheme of optical transitions responsible for the EIT resonance in the hyperfine manifold of ^{87}Rb. In the reference frame associated with the coupling beam, see Fig. 1, the susceptibility tensor has a diagonal structure and in the basis of circular polarizations can be expressed by the following sum [22]:

$$\chi_q^{q'}(\mathbf{r},\Delta_2) = -\delta_q^{q'} \sum_{n(m),m'(m),m} \frac{1}{\hbar} \frac{|(\mathbf{d}\cdot\mathbf{e}_q^*)_{nm}|^2}{\Delta_2 + i\Gamma/2} \rho_{mm}(\mathbf{r}) \times \left\{ 1 - \frac{|V_{nm'}|^2}{\Delta_2 + i\Gamma/2} \frac{1}{\Delta_1 - \Delta_2 + \Sigma_{nm'}(\Delta_2)} \right\}. \tag{2.1}$$

Note that, for notational convenience, we do not explicitly include the detuning Δ_1 in the argument of the susceptibility. Here $(\mathbf{d}\cdot\mathbf{e}_q^*)_{nm}$ represents the transition dipole moments between the lower $|m\rangle \equiv |F,m\rangle$ and upper $|n\rangle \equiv |F',n\rangle$ Zeeman sublevels; $\rho_{mm}(\mathbf{r}) = n_0(\mathbf{r})/(2F+1)$ are the population components of the atomic density matrix, where $n_0(\mathbf{r})$ is the local density of atoms at a spatial point $\mathbf{r}$. In Eq. (2.1) we use standard covariant and contravariant notation for the basis vectors of circular polarizations, see Ref. [26], which can be expressed by Cartesian basis vectors as $\mathbf{e}_0 = \mathbf{e}_z$, $\mathbf{e}_{\pm 1} = \mp(\mathbf{e}_x \pm i\mathbf{e}_y)/\sqrt{2}$ [27].

The first line in Eq. (2.1) is the linear contribution into the susceptibility of the medium and the second line describes the influence of the coupling field and is responsible for the EIT effect. Here $V_{nm'} = \langle n|-\mathbf{d}\cdot\mathbf{E}_c/2\hbar|m'\rangle$ are the transition matrix elements for the coupling mode with amplitude $\mathbf{E}_c$. Quantum states $|n\rangle$ and $|m'\rangle \equiv |F,m'\rangle$ are subsequently chained with an initial state $|m\rangle$ via respective Λ-type excitation channel. This is indicated in the sum by the dependence of the subscripted indices on m: $m'=m'(m)$ and $n=n(m)$. The frequency detunings Δ_1 and Δ_2 are, respectively, the offsets of the coupling and probe modes ω_1 and ω_2 from the resonance $\Delta_{1,2} = \omega_{1,2} - \omega_{F'F}$ with $F=2,1$; $F'=1$. The pole in the denominator of Eq. (2.1) is shifted due to the Autler-Townes effect and the relevant self-energy correction is given by [22]

$$\Sigma_{nm'}(\Delta_2) \equiv \Delta_{nm'}(\Delta_2) - \frac{i}{2}\Gamma_{nm'}(\Delta_2) = \frac{|V_{nm'}|^2}{\Delta_2 + i\Gamma/2}. \tag{2.2}$$

For a monochromatic probe wave propagating in the sample either along or orthogonal to the coupling beam its coherent interaction with the atomic medium is driven by a respective Λ transition shown in the upper diagram of Fig. 2. The phase of the wave is modified by the respective component of the scattering tensor and strongly depends on the polarization type. The wave propagation along arbitrary direction is expressed by the Green's function introduced and discussed in Ref. [22]. If the polarization of incoming wave does not coincide with an eigenmode of the susceptibility tensor the polarization of the outgoing wave can essentially differ from its original type.

The scattering tensor is given by [22]

$$\hat{\alpha}_{pq}^{(m''m)}(\Delta_2) \equiv \alpha_{pq}^{(m''m)}(\Delta_2)|m''\rangle\langle m| = -\sum_{m'(n),n} \frac{1}{\hbar}\frac{(d_p)_{m''n}(d_q)_{nm}}{\Delta_2 + i\Gamma/2}|m''\rangle\langle m| \times \left\{1 - \frac{|V_{nm'}|^2}{\Delta_2 + i\Gamma/2}\frac{1}{\Delta_1 - \Delta_2 + \Sigma_{nm'}(\Delta_2)}\right\}. \quad (2.3)$$

This characteristic, being an operator in atomic subspace, describes the process shown in the lower diagram of Fig. 2. Expression (2.3) determines the amplitude of the outgoing wave for either the elastic or inelastic spontaneous scattering channel accompanied by the atomic transition from the state $|m\rangle \equiv |F,m\rangle$ with $F=1$ to the state $|m''\rangle \equiv |F,m''\rangle$ with $F=1$ (Rayleigh channel) or $F=2$ (inelastic Raman channel). Unlike light scattering from a nondisturbed atom, the scattering process under conditions of EIT resonance is strongly modified by the dressing effect associated with the coupling field.

III. RESULTS

In our numerical calculations we considered as an example ^{87}Rb atoms, where the coupling field and the probe light excitations are respectively applied on the $F=2 \leftrightarrow F'=1$ (empty) and $F=1 \rightarrow F'=1$ (equally populated) hyperfine transitions, as shown in Fig. 2. The coupling field is always right-hand circularly polarized and is on exact resonance, i.e., $\Delta_1=0$. Its amplitude is determined by the Rabi frequency $\Omega_c=2|V_{nm'}|$, which we defined with respect to the $m'=\{F=2,m'=-1\} \leftrightarrow n=\{F'=1,n=0\}$ hyperfine Zeeman transition. Other transition matrix elements are proportional to Ω_c and algebraic factors depending on Clebsch-Gordon coefficients. It is important to note that, in all the results which follow, the absolute numerical values of the susceptibility are scaled by the quantity $n_0\lambda^3$ (n_0 is a local density of atoms and λ is the transition bar wavelength). This means that the values of the various components of the susceptibility tensor (or the complex indices of refraction) may be found directly from the graphs for any experimental conditions.

We begin our consideration of optical anisotropy of atomic ensembles under conditions of EIT with analysis of the forwardly propagating light. For probe light propagating collinearly with a coupling mode the susceptibility of the sample has two orthogonal circularly polarized eigenmodes. The optical anisotropy manifests itself here in their different spectral dependencies, as shown in Figs. 3 and 4. The spectral width of the transparency window for a left-hand circularly polarized probe light (σ_-) is approximately two times wider than that for right-hand (σ_+) one. The slope angles for corresponding dispersion curves also essentially differ.

The differences in susceptibilities cause different absorption and group velocities for light pulses with different circular polarizations. In a steady-state regime, this effect can be implemented for coherent control of polarization rotation for the linearly polarized light under EIT conditions, see Ref. [11]. In the general situation of elliptically polarized and pulsed probe this mechanism can be applied for temporal

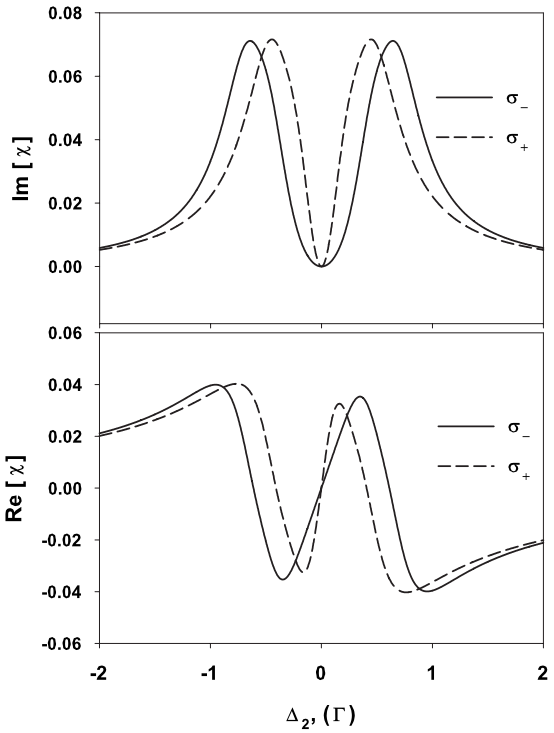

FIG. 3. Real (lower panel) and imaginary (upper panel) parts of the sample susceptibility for left-hand (σ_-) and right-hand (σ_+) circularly polarized probe collinearly propagating with a coupling mode. The susceptibility is scaled in units of $n_0\lambda^3$ (n_0 is a local density of atoms and λ is the transition bar-wavelength) and calculated for the Rabi frequency $\Omega_c=\Gamma$.

separation of the pulse into components of two pulses with orthogonal polarizations. This effect can be specifically important in application to quantum information protocols. It makes possible to transform a single photon polarization qubit into superposition of the photon's fractions separated in

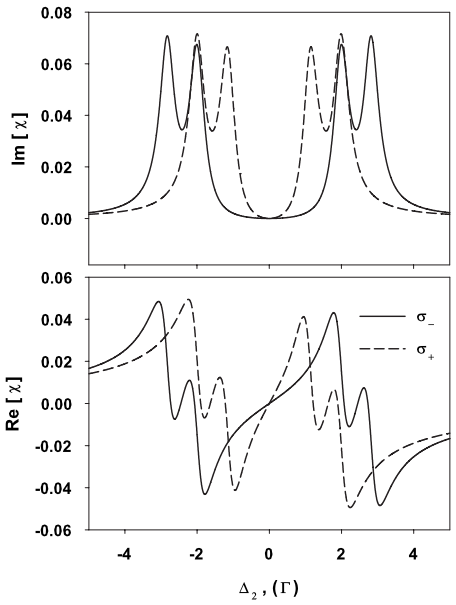

FIG. 4. Same as in Fig. 3 but for the Rabi frequency $\Omega_c=4\Gamma$.

time. In turn this makes technically feasible a further long distance transfer of such a modified quantum bit with a fiber line.

We point out that optical effects associated with the results of Fig. 3 are not small. Under external parameters corresponding to the figure, maximum rotation of a linearly polarized probe beam takes place for a detuning approximately equal to $\pm 0.5\Gamma$. The associated rotation angle is proportional to the resonant optical depth b_0 of the medium (not modified by the EIT effect). The corresponding coefficient is about 7.2° (i.e., the rotation angle is about 145° for $b_0=20$). For a detuning of $1/30\Gamma$, the proportionality factor is about 1.2° (25° for $b_0=20$).

The physical origin of circular dichroism and gyrotropy of the sample in the case under consideration connects with the fact that for a given right-hand polarization the coupling mode is applied to three different transitions $\{F=2,m'=-2\}\leftrightarrow\{F'=1,n=-1\}$, $\{F=2,m'=-1\}\leftrightarrow\{F'=1,n=0\}$, and $\{F=2,m'=0\}\leftrightarrow\{F'=1,n=1\}$, see Fig. 2. The corresponding transition amplitudes have different Clebsch-Gordon factors and therefore different coupling strengths. Thus for collinear geometry there are three uncoupled Λ-type schemes with different transparency windows. The left-hand polarized probe light interacts with the sample through the first two transitions while the right-hand one interacts through the last two of them. As a consequence the left-hand polarized light has a broader spectral window and better conditions for its transport via an EIT channel. This result seems to us important from the point of view of the quantum information applications. It clearly indicates that in a realistic multilevel configuration, associated with any alkali atom, the EIT process, designed for either slow light or quantum memory protocols, should be optimal if the coupling and probe modes are not only spectrally orthogonal but also polarization orthogonal.

The spectral dependence of optical anisotropy under EIT conditions for cold atoms strongly depends on the intensity of the coupling light. In Fig. 4 we show the spectrum of the susceptibility for the case when the Rabi frequency of the coupling visibly exceeds the natural width of the excited states. The dynamic Stark effect manifests itself differently for different transitions and we see a complicated spectral dependence with additional regions of partial transparency. Such spectral behavior of absorption and refraction should be taken into account in the case of a short probe pulse whose spectrum covers all the structure. Various spectral components of the pulse propagate under different conditions which causes essential distortion of the probe pulse. Note that similar features in the probe pulse dynamics was predicted and analyzed earlier for a three level configuration in Ref. [28]. For multilevel systems in the presence of several Zeeman sublevels differently disturbed by the coupling field, this effect becomes even more complicated.

Optical anisotropy of the atomic ensemble makes itself evident also in the fact that properties of a transmitted probe pulse depend on the propagation direction. If the probe light propagates in an arbitrary direction, as is shown in Fig. 1, the susceptibility tensor becomes nondiagonal in a given polarization basis. In the reference frame associated with the probe beam and rotated by Euler angles α,β,γ with respect to the frame associated with the coupling beam, the susceptibility components, defined in the basis of circular polarizations, are given by

$$\tilde{\chi}^{+1}_{+1}(\cdots)=\frac{(1+\cos\beta)^2}{4}\chi^{+1}_{+1}(\cdots)+\frac{(1-\cos\beta)^2}{4}\chi^{-1}_{-1}(\cdots)+\frac{\sin^2\beta}{2}\chi^{0}_{0}(\cdots),$$

$$\tilde{\chi}^{-1}_{-1}(\cdots)=\frac{(1-\cos\beta)^2}{4}\chi^{+1}_{+1}(\cdots)+\frac{(1+\cos\beta)^2}{4}\chi^{-1}_{-1}(\cdots)+\frac{\sin^2\beta}{2}\chi^{0}_{0}(\cdots),$$

$$\tilde{\chi}^{+1}_{-1}(\cdots)=\frac{1}{4}e^{2i\gamma}\sin^2\beta[\chi^{+1}_{+1}(\cdots)+\chi^{-1}_{-1}(\cdots)-2\chi^{0}_{0}(\cdots)],$$

$$\tilde{\chi}^{-1}_{+1}(\cdots)=\frac{1}{4}e^{-2i\gamma}\sin^2\beta[\chi^{+1}_{+1}(\cdots)+\chi^{-1}_{-1}(\cdots)-2\chi^{0}_{0}(\cdots)]. \tag{3.1}$$

The major components of the susceptibility tensor in the right-hand side of these equations are expressed by Eq. (2.1). To avoid any confusion we precisely show the index position for covariant and contravariant notation of the tensor components in the left-hand side. The left-hand side gives us the transverse component of the susceptibility tensor in the local reference frame associated with a probe beam, which are needed to define the Green's propagation function see Ref. [22]. Because of axial symmetry of the problem the susceptibility of the sample is independent on azimuthal angle α. However the coupling between orthogonal modes formally depend on angle γ because of uncertainty in definition of directions of transverse axes in the rotated frame. Without losing of generality this angle can be set as $\gamma=0$ as we will further assume.

The EIT effect becomes strongly modified by its dependence on the angle β between probe and coupling fields wave vectors. The probe pulse with given polarization moving along different directions has different group velocity and is characterized by a different spectral shape of the transparency windows. As follows from Eqs. (3.1) in the case of noncollinear geometry, when the angle between the probe and coupling field wave vectors is not equal to zero, diagonal elements of susceptibility tensor differ as before. However, in this case nondiagonal elements are also nonzero. This means that orthogonal polarization components appear in the transmitted light and the polarization state of the probe light changes when propagating. For example, for an initial circularly polarized beam, the output radiation field is elliptically polarized. The generated orthogonal component is very sensitive to experimental conditions. We demonstrate this in Figs. 5 and 6. In Fig. 5 we show the spectrum of the real and imaginary parts of the non diagonal element of susceptibility tensor for $\beta=\pi/2$ and for one specific value of the coupling field Rabi frequency $\Omega_c=\Gamma$. As one can see there is fine spectral structure of the susceptibility even at a relatively

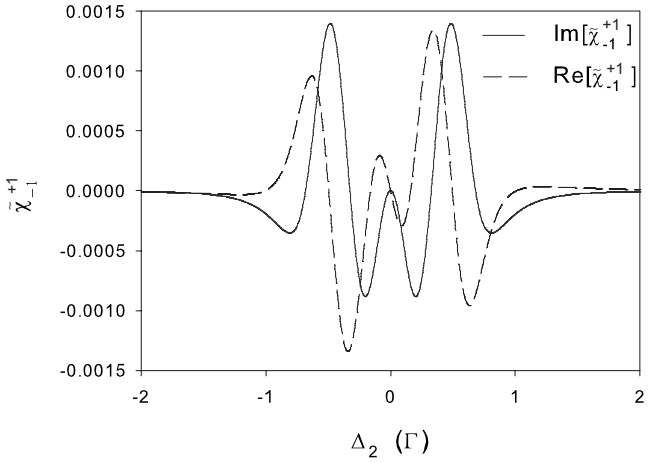

FIG. 5. Real and imaginary part of a nondiagonal component $\tilde{\chi}_{-1}^{+1}$ of the susceptibility tensor scaled in units of $n_0\lambda\!\!\!^{-3}$ (n_0 is a local density of atoms and $\lambda\!\!\!^{-}$ is the transition bar wavelength). The data are obtained for a probe beam orthogonal to the coupling laser propagation direction for $\beta=\pi/2$ and for the Rabi frequency $\Omega_c=\Gamma$. In this geometry the optical properties of the atomic sample are the same for left and right-hand circularly polarized probe light and both diagonal elements of susceptibility tensor coincide.

small Rabi frequency (compare this with dependencies shown in Figs. 3 and 4).

These spectral features become apparent in the dynamics of the orthogonal component, i.e., in the corresponding pulse temporal shape, see Fig. 6. We consider light propagation through the anisotropic medium in the case of an initially right-hand circularly polarized Gaussian-type probe pulse. The light with left-hand circular polarization is observed. Note that for $\beta=\pi/2$ the picture is symmetrical with respect to the type of circular polarization and we have the same results for alternative selection of initial and observed polarizations. The probe pulse duration is chosen large enough so the spectral width of the pulse is less than the width of the transparency windows. In such a way the right-hand circularly polarized component is transmitted through the sample with a certain absorption but practically without shape distortion. At the same time, as is clear from Fig. 6, the shape of the orthogonal component differs essentially from the Gaussian shape of the incoming pulse. In Fig. 6 we show three dependencies calculated for different optical thicknesses (depth) b_0 of the atomic cloud [29]. As follows from the presented results, the intensity of the orthogonal polarization component increases as optical depth increases. The time delay also increases, which is an indication of the slow light phenomenon under EIT effect. Although the time delay is small in absolute terms, it corresponds to a very long spatial delay for both the main and the orthogonal probe channel light pulses. For the external parameters used in our calculations the appearance of the orthogonal component seems as a weak effect. However, let us point out that even being small this effect can be really important if the precise control of the probe pulse polarization would be necessary. This is a typical situation for quantum information protocols.

Let us make the following remark concerning the above results. Strictly speaking for any selected propagation direction the Hermitian part of the susceptibility tensor (3.1) can be always diagonalized in a special basis of eigenvectors with elliptical polarizations to be defined. If incoherent losses were negligible the polarization of the probe transmitted in such an elliptical eigenmode will not be changed in the propagation process under EIT conditions. However, in practice the exact parameters of the system can be unknown. In addition the population of the Zeeman sublevels can be not perfectly homogeneous because of the optical pumping effect, which makes the problem even more subtle and lies out of the scope of the present paper. In such a situation the anisotropy effects, which we discussed for relatively simple homogeneous Zeeman distribution, become actually important as far they can generate uncontrollable change of the probe light polarization.

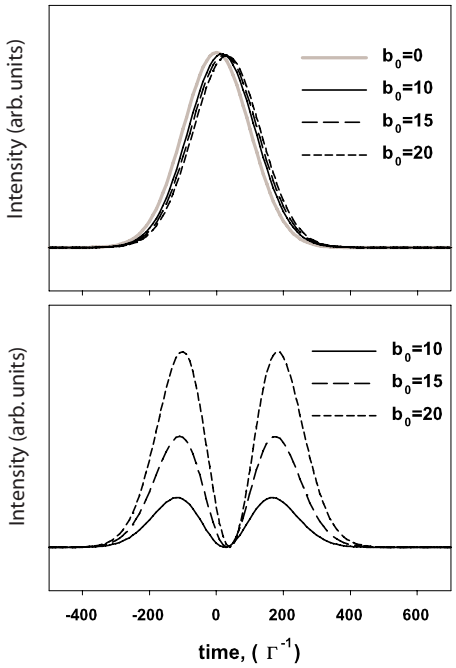

FIG. 6. (Color online) These plots show how the polarization properties of the transmitted pulse are changed if the probe pulse crosses the sample at the direction perpendicular to the control beam. The upper panel displaces the main part of the outgoing pulse in its initial polarization, which can be either right- or left-hand polarized. The lower panel shows the intensity of the probe pulse transmitted the sample in the orthogonal circular polarization. Different curves correspond to different optical depths b_0 of the cloud and the data set corresponds to the Rabi frequency $\Omega_c=\Gamma$. Despite the fact that under external parameters used in this calculation the time delay is small, the temporal points corresponding to the maximum values of the two orthogonal components separate from each other by an interval comparable with the incoming pulse duration.

The polarization properties of light incoherently scattered by an ultracold atomic ensemble are also essentially modified by the presence of the coupling field, see Fig. 2 and discussion in Sec. II B. In Fig. 7 we show how the circular polarization degree for light incoherently scattered in different directions is modified due to the presence of the Autler-Townes structure near atomic resonance. The dependencies shown in Fig. 7 were calculated for a Gaussian-type atomic

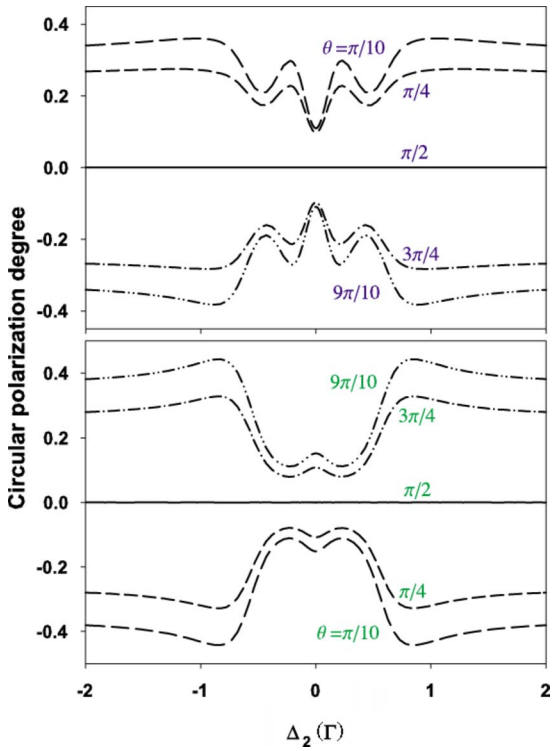

FIG. 7. (Color online) These graphs show how the polarization properties of the scattered light are modified by the presence of the coupling field and by the Autler-Townes structure see Fig. 2. The spectral dependence of the circular polarization degree for light incoherently scattered at different angles θ are shown for the Rayleigh channel (upper panel) and for the Raman channel (lower panel). The spectra were calculated for a Gaussian-type atomic cloud with a peak density of $n_0=16\times10^{10}$ cm^{-3} and a Gaussian radius $r_0=0.1$ cm. The input probe is in a right-hand circularly polarized mode and collinearly propagating with a coupling beam. The coupling field has a Rabi frequency $\Omega_c=\Gamma$.

cloud with a peak density of $n_0=16\times10^{10}$ cm^{-3} and a Gaussian radius $r_0=0.1$ cm. The input probe light is assumed to be right-hand circularly polarized and propagating collinearly with the coupling beam.

From the curves in Fig. 7 one can see that the coupling field changes the polarization properties of the scattered light both for the Rayleigh- and the Raman-scattering channels. Depolarization through multiple scattering is enhanced in the region of the EIT resonances. Physically, this connects with the fact that in the noncollinear scattering geometry there are various possible Λ-type transitions participating in the process. In each scattering event they contribute coherently and cannot be separated from each other, as shown in Fig. 2. As a consequence, the scattering tensor has a complicated internal spectral structure. The change in the polarization of light takes place in every scattering event and in addition also during the propagation between two such successive events in the medium. A relatively strong coupling field has action upon both of these processes and generates such complex polarization spectra as shown in Fig. 7.

IV. SUMMARY

In summary, we have developed a realistic treatment of light propagation in an inhomogeneous ultracold atomic gas sample under conditions of electromagnetically induced transparency. We particularly have focused on the polarization dependence of the optical properties of the medium. In the present case we have considered not only the transmitted light, but also the diffusely scattered light in the medium. The calculated results display the essential importance and rich phenomenology of the polarization effects in both the time and frequency domain. This globally results in great quantitative and even qualitative difference with predictions of Λ-configured model descriptions. Some effects may be of particular importance in managing the fidelity of pulse storage and retrieval in light storage and quantum memory applications. Extensive exploration of the multifaceted parameter space, necessary in order to identify the most desirable collection of variables for optimizing transmission of probe pulses, remains the subject of future research.

ACKNOWLEDGMENTS

We appreciate the financial support of the Russian Foundation for Basic Research (Grant No. RFBR-05-02-16172-a), by INTAS (Project No. 7904), and the National Science Foundation (Grant No. NSF-PHY-0355024).

[1] J. P. Marangos, J. Mod. Opt. **45**, 471 (1998).
[2] M. D. Lukin, Rev. Mod. Phys. **75**, 457 (2003).
[3] M. Fleischhauer, A. Imamoglu, and J. P. Marangos, Rev. Mod. Phys. **77**, 633 (2005).
[4] F. S. Pavone, G. Bianchini, F. S. Cataliotti, T. W. Haensch, and M. Inguscio, Opt. Lett. **22**, 736 (1997).
[5] S. Wielandy and A. L. Gaeta, Phys. Rev. Lett. **81**, 3359 (1998).
[6] D. McGloin, M. H. Dunn, and D. J. Fulton, Phys. Rev. A **62**, 053802 (2000).
[7] T. H. Yoon, C. Y. Park, and S. J. Park, Phys. Rev. A **70**, 061803(R) (2004).
[8] D. Cho, J. M. Choi, J. M. Kim, and Q. Han Park, Phys. Rev. A **72**, 023821 (2005).
[9] A. V. Durrant, H. X. Chen, S. A. Hopkins, and J. A. Vaccaro, Opt. Commun. **151**, 136 (1998).
[10] G. G. Kozlov, E. B. Aleksandrov, and V. S. Zapasski, Opt. Spectrosc. **97**, 909 (2004).
[11] B. Wang, S. Li, J. Ma, H. Wang, K. C. Peng, and M. Xiao, Phys. Rev. A **73**, 051801(R) (2006).
[12] G. S. Agarwal and S. Dasgupta, Phys. Rev. A **67**, 023814 (2003).
[13] V. A. Sautenkov, Y. V. Rostovtsev, H. Chen, P. Hsu, G. S. Agarwal, and M. O. Scully, Phys. Rev. Lett. **94**, 233601 (2005).
[14] S. D. Jenkins, D. N. Matsukevich, T. Chanelière, A. Kuzmich,

and T. A. B. Kennedy, Phys. Rev. A **73**, 021803(R) (2006).
[15] D. N. Matsukevich, T. Chanelière, S. D. Jenkins, S.-Y. Lan, T. A. B. Kennedy, and A. Kuzmich, Phys. Rev. Lett. **96**, 033601 (2006).
[16] L. V. Hau, S. E. Harris, Z. Dutton, and C. H. Behroozi, Nature (London) **397**, 594 (1999).
[17] A. M. Akulshin, A. A. Celikov, and V. L. Velichansky, Opt. Commun. **84**, 139 (1991).
[18] C. Y. Ye and A. S. Zibrov, Phys. Rev. A **65**, 023806 (2002).
[19] P. R. S. Carvalho and E. E. Luis de Araujo, and J. W. R. Tabosa, Phys. Rev. A **70**, 063818 (2004).
[20] M. Fleischhauer, Europhys. Lett. **45**, 659 (1999).
[21] A. B. Matsko, I. Novikova, M. O. Scully, and G. R. Welch, Phys. Rev. Lett. **87**, 133601 (2001).
[22] V. M. Datsyuk, I. M. Sokolov, D. V. Kupriyanov, and M. D. Havey, Phys. Rev. A **74**, 043812 (2006).
[23] D. V. Kupriyanov, I. M. Sokolov, C. I. Sukenik, and M. D. Havey, Laser Phys. Lett. **3**, 223 (2006).
[24] To set our terminology, we refer in brief to Rayleigh- and elastic Raman-scattering processes as Rayleigh scattering. The terminology Raman scattering refers only to hyperfine inelastic Raman scattering.
[25] D. V. Kupriyanov, I. M. Sokolov, and S. V. Subbotin, Sov. Phys. JETP **66**, 71 (1987).
[26] D. A. Varshalovich, A. N. Maskalev, and V. K. Khersonskii, *Quantum Theory of Angular Momentum* (World Scientific, Singapore, 1988).
[27] It is important to recognize that, in this complex basis set, the contravariant basis vectors are given by $\mathbf{e}^q=\mathbf{e}_q^*$ and the metric tensor has a nondiagonal form $(\mathbf{e}_q)_p=(-)^q\delta_{q-p}$ such that a right-hand polarization vector with $q=+1$ has negative covariant projection with $p=-1$.
[28] R. N. Shakhmuratov and J. Odeurs, Phys. Rev. A **71**, 013819 (2005).
[29] For a Gaussian atom distribution in the trap, the weak-field optical depth, on resonance and through the center of the trap is given by $b_0=\sqrt{2\pi}n_0\sigma_0 r_0$, where n_0 is the peak density and σ_0 is the normal (not modified by the EIT effect) resonance cross section, r_0 is the Gaussian radius of the cloud.